MicroSurf: Guiding Energy Distribution inside Microwave Oven with Metasurfaces

Yiwen Song*
Carnegie Mellon Unversity
Pittsburgh, PA, USA
yiwens2@andrew.cmu.edu

Hao Pan†
Microsoft Research Asia
Shanghai, China
panhao@microsoft.com

Longyuan Ge*
Shanghai Jiao Tong University
Shanghai, China
gly2000@sjtu.edu.cn

Lili Qiu
Microsoft Research Asia
The University of Texas at Austin
Shanghai, China
liliqiu@microsoft.com

Swarun Kumar
Carnegie Mellon University
Pittsburgh, PA, USA
swarun@cmu.edu

Yi-Chao Chen
Shanghai Jiao Tong University
Shanghai, China
yichao@sjtu.edu.cn

Abstract

Microwave ovens have become an essential cooking appliance owing to their convenience and efficiency. However, microwave ovens suffer from uneven distribution of energy, which causes prolonged delays, unpleasant cooking experiences, and even safety concerns. Despite significant research efforts, current solutions remain inadequate. In this paper, we first conduct measurement studies to understand the energy distribution for 10 microwave ovens and show their energy distribution in both 2D and 3D is very skewed, with notably lower energy levels at the center of the microwave cavity, where food is commonly placed. To tackle this challenge, we propose a novel methodology to enhance the performance of microwave ovens. Our approach begins with the development of a measurement driven model of a microwave oven. We construct a detailed 3D model in the High Frequency Structure Simulator (HFSS) and use real temperature measurements from a microwave to derive critical parameters relevant to the appliance's functionality (*e.g.*, operating frequency, waveguide specifications). We then develop a novel approach that optimizes the design and placement of a low-cost passive metasurface for a given heating objective. Using extensive experiments, we demonstrate the efficacy of our approach across diverse food, optimization objectives, and microwave ovens.

CCS Concepts

• **Hardware** → **Wireless devices**; • **Human-centered computing** → *Ubiquitous and mobile devices.*

ACM Reference Format:
Yiwen Song, Hao Pan, Longyuan Ge, Lili Qiu, Swarun Kumar, and Yi-Chao Chen. 2024. MicroSurf: Guiding Energy Distribution inside Microwave Oven with Metasurfaces. In *The 30th Annual International Conference on Mobile Computing and Networking (ACM MobiCom '24), November 18–22, 2024, Washington D.C., DC, USA.* ACM, New York, NY, USA, 15 pages. https://doi.org/10.1145/3636534.3690697

1 Introduction

Microwave ovens are ubiquitous kitchen appliances. According to the United States Department of Agriculture, over 90% of households in the United States own microwave ovens [1]. However, the convenience of microwave ovens comes with a number of well-known drawbacks. During the microwave heating process, "cold spots" can be left behind, which can lead to the survival of harmful bacteria and other pathogens that may cause foodborne illnesses, increasing the risk of food poisoning [1]. Uneven heating can also cause "hot spots", which can increase the risk of burns to the mouth and throat when consuming the food. Furthermore, many people have experienced eggs exploding in the microwave, which is also mainly due to uneven heating [40].

The uneven heating in a microwave oven stems from its unique heating mechanism, where it produces high-powered radio-frequency (RF) electromagnetic (EM) waves that heat food via dielectric heating [26, 38]. The EM waves inside the microwave oven tend to form standing waves [16]. At the wave nodes, the amplitude is consistently zero, resulting in no heating. This means that food positioned at these nodal points will remain cold. Conversely, at the antinodes,

*Yiwen Song and Longyuan Ge did this work as interns at Microsoft Research Asia (Shanghai).
†Hao Pan is the corresponding author.

Permission to make digital or hard copies of part or all of this work for personal or classroom use is granted without fee provided that copies are not made or distributed for profit or commercial advantage and that copies bear this notice and the full citation on the first page. Copyrights for third-party components of this work must be honored. For all other uses, contact the owner/author(s).
ACM MobiCom '24, November 18–22, 2024, Washington D.C., DC, USA
© 2024 Copyright held by the owner/author(s).
ACM ISBN 979-8-4007-0489-5/24/11
https://doi.org/10.1145/3636534.3690697

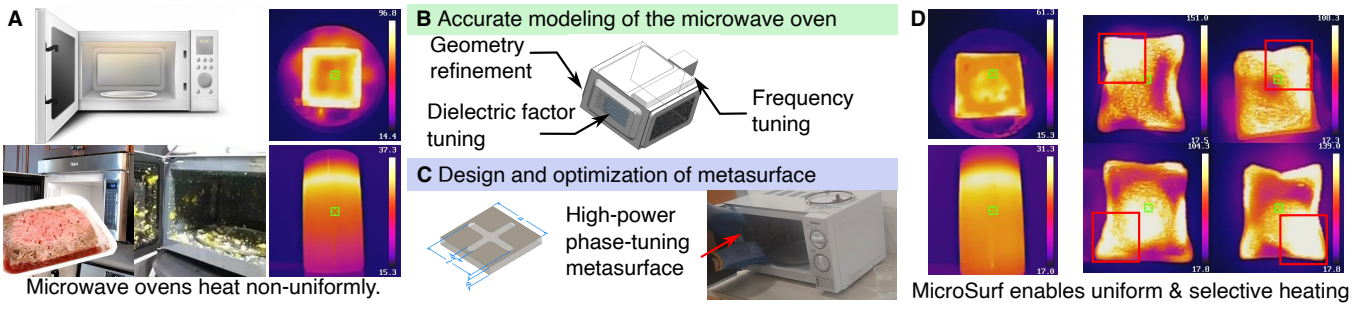

Figure 1: System Overview: (A) Microwave ovens naturally heat non-uniformly due to uneven electric field distribution inside the oven chamber. MicroSurf guides the microwave energy by (B) accurate modeling of the microwave oven, and (C) designing and optimizing a metasurface that works in a high-power environment that phase-tunes the waves inside to change the standing wave distribution. (D) MicroSurf enables uniform heating of different food objects and can further achieve selective heating in different food corners.

food can heat up much more rapidly. This discrepancy between nodes and antinodes leads to the uneven heating of food, with some areas being overheated while others remain underheated.

Various efforts have been made in both industry and research to more evenly distribute heat. The most common solution is a turntable that constantly rotates food inside the microwave oven. Another option is to use a stirrer. It is a fan-like device that rotates in front of the electric field emitter, changing the initial propagation direction of the EM waves. Our measurements from 10 different microwave ovens show that even with the turntables or the stirrers, the heat distribution inside the microwave oven is still uneven both horizontally and vertically. More recently, software-defined cooking (SDC) [15] proposes a closed-loop control of the turner to achieve desired thermal patterns. It requires significant modifications to the microwave oven: adding neon light arrays to sense EM field, using an IR camera to record lamp flashes, replacing a low-cost turntable motor with a more expensive step motor controlled by an Arduino board, and adding microwave shields at specific locations. These modifications are challenging to deploy in practice. Moreover, SDC only optimizes 2D heat distribution since it requires neon lights to be placed on the hot surface to measure power levels. However, real heating scenarios require controlling heat distribution in 3D, which SDC does not address.

This paper addresses the following question: Can we make a low-cost, easy-to-deploy device to control the 2D or 3D heat distribution inside a microwave oven to achieve different heating objectives? We present MicroSurf, an effective yet low-cost solution to control the EM energy inside a microwave oven by placing one or more passive metasurfaces inside the oven chamber, as shown in Figure 1. We choose passive smart surfaces rather than more sophisticated electronics since they cannot withstand the thousand-watt power levels inside a microwave oven. We first develop an empirical model of a microwave oven using a combination of a detailed 3D model construction, EM simulation, and parameter refinement techniques. We then carefully design and refine the surfaces to resonate with the EM waves, and therefore change the standing wave inside the oven chamber. We realize the desired energy distribution by changing the configuration and placement of the surfaces. We implement and evaluate MicroSurf to demonstrate our approach can effectively optimize different heating objectives for fluids and solids across 2D or 3D areas, including uniformly heating water, milk, bread, and meat, as well as focusing energy at 4 corners of the bread.

While metasurfaces have been recently explored extensively at 2.45 GHz [34], primarily for communication and sensing applications [18, 43], they are ill-suited to the microwave oven context, which is extremely high-power (800-1600 W vs. few W at most for communication or sensing applications) and the unique propagation patterns within the oven that induces standing waves. Indeed, placing prior metasurfaces within a microwave oven would incur safety concerns due to the sparks induced by metallic edges or small gaps. MicroSurf therefore seeks to address two design questions detailed below:

(1) How to accurately model EM distribution inside the microwave oven?: While simple models for microwave propagation, such as the cavity resonator model [11, 25, 33], have been considered, the complex geometry of real-world microwaves result in considerable deviations from these models. Indeed, we find that even after we construct a detailed 3D model of a microwave oven using the High-Frequency Structure Simulator (HFSS), there is a significant deviation between the estimated energy distribution from HFSS versus the measured distribution using a thermal camera. Through careful investigation, we identify that several real-world

factors play a role, such as operating frequency offsets, diverse heating properties across different objects, as well as CAD model meshing defects. Sec. 4 shows how MicroSurf adapts the microwave model to account for these real-world complications by identifying the variables that most affect the simulated EM field distribution, and then using a Bayes search to determine these parameters of the microwave oven.

(2) How do we design Microwave-Compatible Metasurfaces?: After determining the microwave oven model, MicroSurf's metasurface element is designed to resonate with the operating frequency of the microwave oven to control EM field distribution. We identify several unique criteria for the metasurface elements to operate inside a microwave oven: (1) They should not include rough edges that build up high electric potential in a high-power microwave environment and may cause sparks. (2) The element is designed to be substrate-free to enhance heating efficiency, as well as avoid burning of the substrate. The substrates can easily get heated or even cause discharge, which wastes power and causes safety concerns. (3) The metasurface should have sufficient control of the phase of the traveling EM waves [19] (*e.g.*, >180 degrees). Sec. 5.2 shows how we achieve these criteria using metasurface elements that are smoothed-edge cross structures with a phase-tuning capability that can be adapted to different microwave ovens with different geometries. We further leverage our RF model of the microwave oven to optimize these metasurfaces in terms of placement and configuration in Sec. 5.3 to achieve desired heating objectives – e.g. uniform heating or focusing energy at specific spots. We envision that a user can choose their desired heating objective by pressing a button on the microwave panel, which will move the metasurface to an appropriate position.

We implement and evaluate the metasurface design using steel-fabricated metasurface sheets and 4 commodity microwave ovens. Our custom-made metasurface costs $4, which can be reduced by several factors with mass production. Our evaluation results show our system is effective in optimizing for different objectives, food, and microwave ovens.

Our contributions can be summarized as follows:

- We develop a measurement-driven model of a microwave oven. We construct a 3D model of a microwave oven and use temperature measurement to derive critical parameters of the microwave. Our model can accurately capture the propagation of EM waves inside the microwave oven.
- We cast the design of a metasurface for achieving a specific heating distribution as an optimization problem. We can support different optimization objectives, such as uniform heating or maximized heating in one or more region(s). We leverage a finite element EM simulator and employ hyperparameter tuner and gradient descent methods to optimize the design and placement of one or more passive metasurfaces.
- We empirically demonstrate the accuracy of our model and the effectiveness of our metasurface design in commodity microwave ovens. Our results show our method increases the temperature by 2-10°C and reduces the temperature standard deviation by 1/5 to 1/2 across different foods.

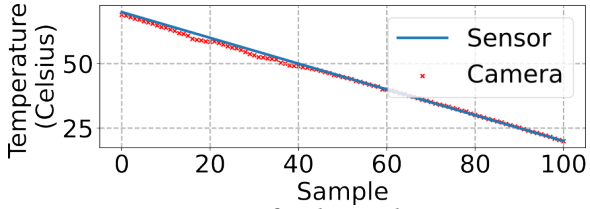

Figure 2: Measurement of a thermal camera compared to a thermometer of 100 points.

2 Preliminaries

2.1 Microwave Oven Heating Principle

Dielectric heating principle: In a microwave oven, food is heated by quickly-alternating the electric field. A microwave oven produces a strong, rapidly changing EM wave inside a metallic chamber. When the EM wave propagates through the food, the small polar molecules inside the food (particularly water) get polarized and rotate, trying to align themselves with the electric field. As the electric field keeps changing, the water molecules rotate and collide with each other. The collision between molecules produces heat, and as the heat transfers to other molecules, the entire piece of food gets heated. This process is called dielectric heating [8].

Speed of Heating: The temperature rise of a specific food region is dependent on the strength of the local electric field. A stronger electric field passes more power to the molecules and thus, brings faster heating. Studies have shown that the overall power absorbed by a homogeneous material is proportional to the square of the electric field intensity [31]. Therefore, the uneven power distribution inside a microwave oven is due to the uneven electric field distribution inside the microwave oven.

2.2 Power Distribution in Microwave Ovens

The power distribution within a microwave is dictated by standing waves that form inside. The microwave oven, with 6 surrounding conductive surfaces constituting a near rectangular cuboid that encircles a chamber, can be abstracted as a cavity resonator [33]. The EM field inside the cavity forms standing waves, which consist of nodes and anti-nodes. Due to the standing waves forming inside the microwave oven, it is challenging to make the electric field distribute equally inside the microwave oven chamber.

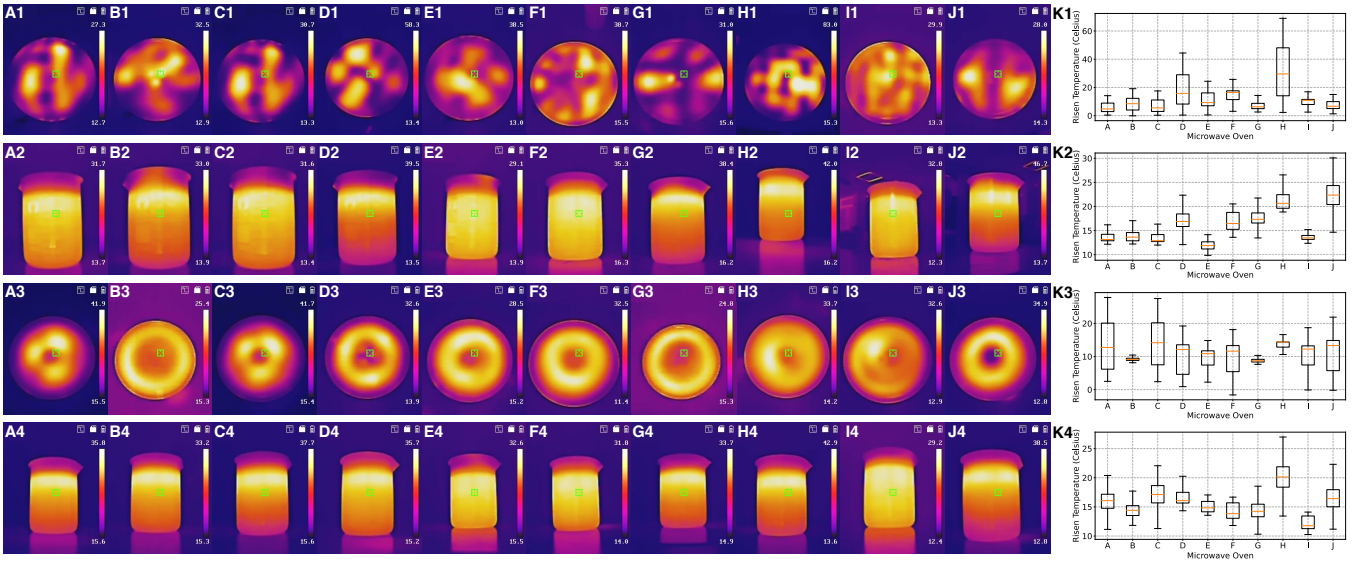

Figure 3: Heat distribution maps collected from 10 different microwave ovens from different brands and models (A-Toshiba, B-Galanz, C-Midea, D-Panasonic, E-Whirpool, F-Midea, G-Panasonic, H-Haier, I-Galanz, J-Galanz). The first row represents the planar heat distribution on the plate with no loads. The second row represents the vertical heat distribution of 50 mL of water heated at the center of the microwave oven. The third row demonstrates the heat distribution on the plate when the plate is rotating. The last row demonstrates the heat distribution of 50 mL of water when the plate is rotating. It can be seen that the microwave oven produces nonuniform heating on the x,y,z-axis. (K) Statistics of the plate or water heat distribution on the horizontal plane or the vertical axis.

We measure existing microwave ovens to understand their power distribution. Conventional measurement methods using antennas or power harvesters [41] are challenging to use inside a microwave because they can only measure the power at specific points instead of the whole surface. Therefore, we use the temperature distribution captured by a thermal camera to estimate the power distribution inside the microwave oven. We validate the accuracy of the thermal camera by comparing its reading with a thermometer. As shown in Figure 2, the readings from the thermal camera closely match those from the thermometer: within ±1 degree.

There is no technology to provide real-time 3D heat distribution inside objects. Therefore, we take thermal images horizontally and vertically. Specifically, the power distribution on the X-Y plane is captured by the temperature distribution on the glass plate, and the power distribution on the X-Z plane is captured by the temperature distribution of a beaker of water. We conduct measurement across multiple microwave ovens (Fig.3). For the microwave ovens of the same model (Fig. 3A), we tested four samples, which all share the same distribution. Microwave ovens of different models may have the same distribution (*e.g.*, in Fig.3AC two microwaves from two brands share the same design and E-field distribution), but in most cases, microwave ovens of different models are likely to have different distributions. Our result in Fig.10 shows consistency across different microwave ovens.

We first deactivate the turner inside the microwave ovens. We turn on the microwave ovens for 60 seconds. Figure 3 (A1-J1) shows the temperature distribution of the glass plate. As we can see, the power distribution is very skewed across all 10 ovens. Figure 3 (K) further shows the temperature distribution using a box plot, where the middle red line corresponds to the mean temperature, and the box length corresponds to the deviation. As we can see, the maximum and minimum temperatures range between 18 – 66 degrees in the horizontal dimension. Figure 3 (A2-J2) further shows the temperature distribution for the water of height 7 cm inside a 50 mL beaker after heating for 30 seconds. We observe significant temperature variation ranging between 3 – 15 degrees in the vertical dimension.

We further activate the turner. Figure 3 (A3-J3) shows the power distribution is less skewed with the turner on. Yet, the centers have significantly lower temperatures than the surroundings as expected. The temperature increase near the center is smaller than that in the surroundings. Meanwhile, the temperature still varies between 4 – 25°C in the horizontal dimension. The temperature variation remains in the vertical dimension, as well, with the temperature range spanning across 3 – 15 degrees.

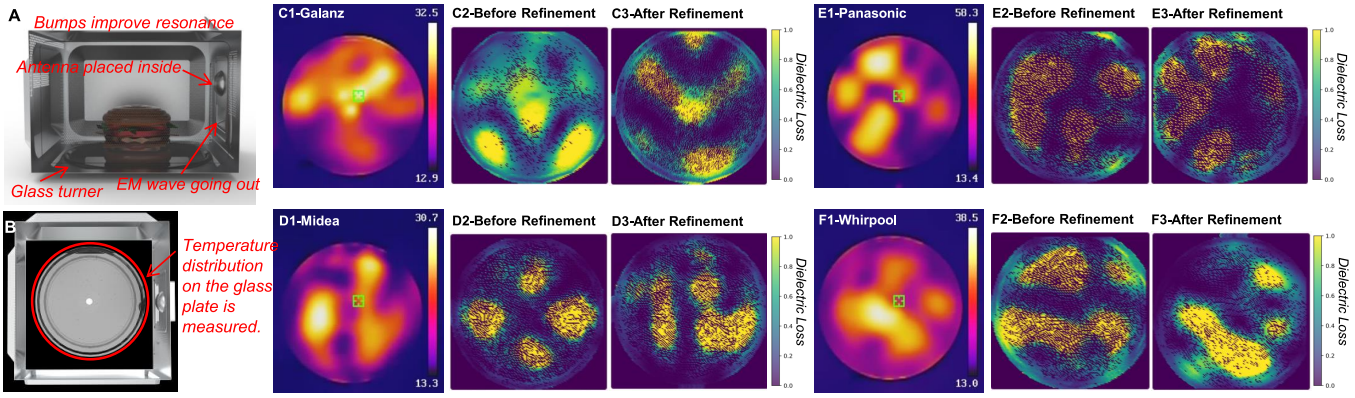

Figure 4: Modeling of the microwave oven: (A) A CAD model of the microwave oven is created on the actual measurements of the microwave oven. A glass turner holds food in the main chamber. A side chamber containing an antenna acts as the EM wave generator. (B) EM wave forms a standing wave inside the microwave oven chamber, where the power distribution is uneven. To measure the power distribution, we measure the temperature distribution on the glass plate. (C)-(F) A comparison of the measured temperature and the fitted dielectric loss.

3 System Overview

MicroSurf optimizes the design, configuration, and placement of passive metasurfaces inside a microwave oven through the following three key steps. First, we develop an accurate microwave model based on empirical measurements. We determine the key microwave parameters that affect the EM field distribution the most by minimizing the error between the estimated power distribution and measured temperature distribution. Second, we identify several key requirements and guidelines for designing metasurfaces for microwave ovens. Third, we develop an effective optimization framework for metasurface design and placement. Our framework is flexible in supporting different objectives, food types, and microwave ovens.

4 Accurately Modeling the Microwave Oven

We need to accurately simulate the electric field inside the microwave oven. If simulation matches reality, what we optimize in simulation is what can be achieved in reality. To close the gap between simulation and reality, we use real measurements to tune the simulation parameters to make the simulated temperature distribution match the real measurements. We model and validate five microwave ovens of five brands – Galanz, Toshiba, Midea, Panasonic, and Whirpool, as shown in Figure 4. The Midea oven and the Toshiba oven yield similar measurements and parameters since they share the same oven design and glass plate.

Establishing 3D CAD models of the microwave oven: We first take measurements of different parts of the microwave ovens and make 3D models in CAD that fit the geometry of the actual microwave ovens shown in Figure 4(A). The microwave oven consists of several major parts that affect heating. **The main chamber** is where the EM waves form standing waves, and where the food is placed. A glass turner lifts and rotates the food. The manufacturer usually deliberately designs physical bumps in the main chamber to improve EM resonance behavior and try to improve efficiency and uniformity. **A waveguide chamber** is on the right side of the microwave oven, where the antenna is placed inside. The waveguide chamber creates near-field coupling with the antenna and re-shapes the transmission from the antenna to the main chamber. The wave exits the waveguide chamber to the main chamber through an opening that is usually covered by a piece of a thin quartz sheet. **The antenna** is the signal source that is placed inside the waveguide chamber. It emits single-frequency EM waves that are generated by a magnetron, which creates high-power resonating voltage at a specific frequency with AC power. The microwave oven manufacturers also make **small holes** on boundaries to help heat dissipation, as well as enable the users to observe the status of the food being heated. The diameters of the holes are designed to be much smaller than one wavelength, 12.24 cm, to prevent leakage. The holes can cause power loss and scattering, and are therefore included in the model.

EM simulation setup and observed deviations: We then use a high-fidelity electromagnetic simulation – Ansys HFSS, to simulate electric fields, as shown in Figure 4(B). We further use Ansys Icepak to take into account heat propagation and heat loss to derive the temperature distribution on the plate.

However, despite careful modeling informed by the oven's specifications, we observe that the simulation does *not* match with the actual temperature measurements. There are three

main reasons that account for the discrepancy, which primarily stem from real-world complications of the microwave oven. First, the actual operating frequency deviates from the 2.45 GHz, where most microwave ovens claim to be operating. This is because the magnetron does not accurately operate at 2.45 GHz. Second, the dielectric factor of the glass plate affects the absorption and reflection of the EM wave, and thus affects the field distribution. The glass plates used by different brands are from different manufacturers, and produce different heating distributions. Third, small measurement and modeling errors of the antenna can affect the radiation pattern of the antenna. Since the standing wave forms inside the main chamber, the radiation pattern offset can lead to a non-negligible offset in the electric field distribution.

Tuning the model: We fine-tune the model to account for the three factors. We make two design decisions during fine-tuning: selecting an appropriate cost function and an appropriate optimization method. The cost function captures the difference between simulation vs. real measurements. Ideally, the cost function must be resilient to measurement noise (*e.g.*, two different measurements from the same oven are compared against the model). Our methodology supports multiple error metrics. We choose peak signal-to-noise-ratio (PSNR) because it is empirically better. To compare HFSS field output results with infrared pictures from a thermal camera, we cut and rescale the infrared images of the plates to 128×128 matrices, where each pixel corresponds to the temperature in a 1 mm^2 resolution. It is compared with the dielectric loss, which symbolizes the energy absorption rate for a unit volume. The HFSS dielectric loss field is also projected into a 128×128 pixel matrix by averaging the corresponding dielectric loss values inside each pixel. The two matrices are normalized through dividing by their respective maximum values. The PSNR value is then calculated by comparing the two 128×128-pixel matrices.

We use NNI [24] to optimize the parameters. We use PSNR as the cost measure, which is calculated as

$$\text{PNSR} = -10\log_{10}\left(\frac{1}{128\times 128}\sum_i\sum_j[M_0(i,j)-M_1(i,j)]^2\right), \tag{1}$$

and where M_0 is the normalized measured temperature matrix and M_1 is the normalized simulated dielectric loss matrix. Since there are multiple parameters and the optimization is non-convex, we use simulated annealing with multiple different starting points to obtain the solution. For each round of optimization, the algorithm returns a set of parameters, which are fed into the HFSS simulation software by the PyAEDT interface, and the HFSS runs and provides the dielectric loss distribution on the plate, which corresponds to the energy absorption rate. The algorithm then computes the PSNR and generates a new set of parameters to be tested.

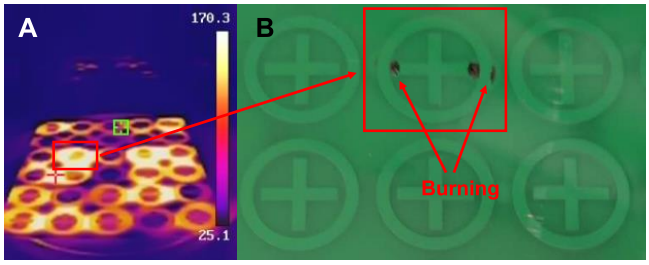

Figure 5: Metasurfaces used in microwave ovens cannot contain substrates, as substrate materials heat up quickly, wasting energy and posing safety risks due to burning and sparking

Results: Figure 4(C)-(F) show the optimization result. For each pair of figures, the left is a measured temperature distribution on the plate, and the right is the simulated dielectric loss distribution. The PSNR values are (C) Galanz – 12.6 dB, (D) Midea/Toshiba – 10.8 dB, (E) Panasonic – 9.9 dB, and (F) Whirpool – 13.1 dB.

5 Metasurface Design

MicroSurf's metasurfaces are smart surfaces that contain an array of patterned conductive elements. By tuning the parameters of the metasurface elements, the elements will have different phase-tuning capabilities. The metasurface can change the amplitude, phase, transmission direction, and beam concentration of the EM waves. Since the microwave oven is a high-power and resonant near-field environment, MicroSurf provides a unique design that optimizes metasurfaces to control the EM field distribution inside the oven. This optimization includes phase modulation of the metasurface design to maximize heating efficiency and/or minimize spatial variation of electric field energy distribution.

5.1 Design Requirements

Different from metasurfaces for communication and sensing, our metasurface inside the microwave oven must meet several unique design criteria in order to guarantee safety, promote efficiency, and provide good performance.

5.1.1 *Choice of passive metasurface*

High safety: Safety in microwave oven operation is important. Placing metallic objects with rough or sharp edges may cause fire or explosive hazards. Our design avoids potential hazards by designing and testing the metasurface inside different microwave ovens and with different foods. To ensure safety, we recommend future designs follow our design guidelines, fabricate using industrial standards and methods rather than DIY, and test using a low heating power and short heating time first and use a thermal camera to capture

the post-heating image to examine if there are any abnormal points of high temperature.

We design a passive metasurface to optimize the EM field distribution in the microwave oven due to its high safety. Although active metasurfaces [5, 17, 30] have been a popular design choice for communication and sensing, the transistors, diodes, capacitors, small pads and thin signal wires can all get burnt by the high power. To ensure the safety of the microwave oven, we use a passive metasurface instead of active metasurfaces. By designing different sets of metasurface elements, we can adjust the phase of EM waves in the microwave oven cavity to achieve uniform heating of food.

The metasurfaces must be designed to prevent burning or sparkling. Microwave oven producers usually warn users not to put metallic objects into the microwave ovens. This is because metallic objects with rough edges and multiple objects touching each other may lead to edge effect [4, 9], which generates extremely high electric field that can cause sparkles or fire. Therefore, to address these safety concerns, the metasurface elements should not contain rough edges. Meanwhile, the gap between metals needs to be larger than 6 mm according to our measurements. Finally, during the fabrication of the metasurfaces, rough edges, scratches, and crevices must be avoided.

Adjustability: However, the passive metasurface cannot be modified after fabrication. To support heating food of different shapes and types, we use the metasurface placement as the control knob. Since standing waves are formed inside the microwave oven, small movements of the metasurface can lead to changes in the EM field distribution. Therefore, before heating different foods, we can place the metasurface in the designated position to achieve uniform heating of the target food.

Substrate-less design support: Metasurfaces usually consist of substrate and metal. However, through extensive measurements, we find that the substrate can absorb heat and reduce the energy efficiency. Figure 5 shows an example of temperature on the metasurface with and without a substrate. It is evident that adding substrate increases temperature, which may lead to burning and sparkling as the substrate can get heated up. Therefore, we seek a design without a substrate. Since the metasurface is substrate-free, all the patterns on the metasurface must be topologically connected.

5.1.2 Compatibility with EM waves in Microwave Ovens

Polarization: The EM wave propagating inside the microwave oven chamber is different from that in communication and sensing. Dipole and patch antennas are used in communication and sensing systems, which produce plane waves with fixed polarization. In contrast, in the microwave oven, the electric field oscillates along different directions. Therefore, to enable 3D tuning capability, the metasurface has to respond to the electric field coming from different directions. To realize this property, the metasurface pattern is designed to be symmetric to achieve isotropic resonance behavior for incident waves with different polarizations.

Co-design with oven chamber: The phase tuning capability of a passive metasurface resonates with the oven chamber and creates different EM field distributions inside the microwave oven. It is well known that the geometry of a cavity resonator determines its energy efficiency when operating at a specific frequency [35]. Therefore, metasurface design and placement should be optimized for a given oven chamber.

5.2 Element Design

A key design decision is to determine if the metasurface should be a reflecting or penetrating metasurface. Ideally, if the metasurface is lossless (*i.e.*, the power sum of reflected and transmitted waves equals to the incident wave), the total power in the heating area is the same regardless of the reflection or transmission ratio. In practice, a transmissive metaruface incurs more energy loss. Therefore, we design a reflecting metasurface.

We find a metallic template that resonates at 2.45 GHz (the operating frequency) and provides 2π phase control. We then use the requirement of standing waves to initialize the metasurface. Finally, we use HFSS, a high-fidelity simulator, to refine our design and optimize our objective inside a given microwave oven. Since our objective is non-linear and the quality of the solution is sensitive to the initial value, we use initialization and refinement to significantly improve the quality and speed of our optimization.

Find resonant geometry: We search for a unit cell that resonates at 2.45 GHz and offers 2π phase control by using the Ansys Electronics HFSS solver to numerically simulate a metasurface. As stated in Sec. 5.1, owing to safety requirements (*e.g.*, to avoid sparks), (i) the unit cell structure should be centrosymmetric, (ii) the maximum distance between metallic parts should be at least 6 mm, and (iii) the patterns need to be topologically connected as there is no substrate to glue disjoint pieces together. We deliberately avoid using thin lines since parallel thin lines easily interact with the 2.45 GHz EM waves and could get heated up quickly [37]. We also avoid using complex resonate-ring structures [12] that creates isolated islands, which are not feasible for substrate-free designs.

With a constrained design space, we select a simple yet effective cross-resonator structure as depicted in Figure 6(A). The surface has two layers: The first layer consists of a hollow cross element, and the second layer is a metallic board to ensure near perfect reflection. We round the edges of the cross. MicroSurf chooses this design for multiple reasons:

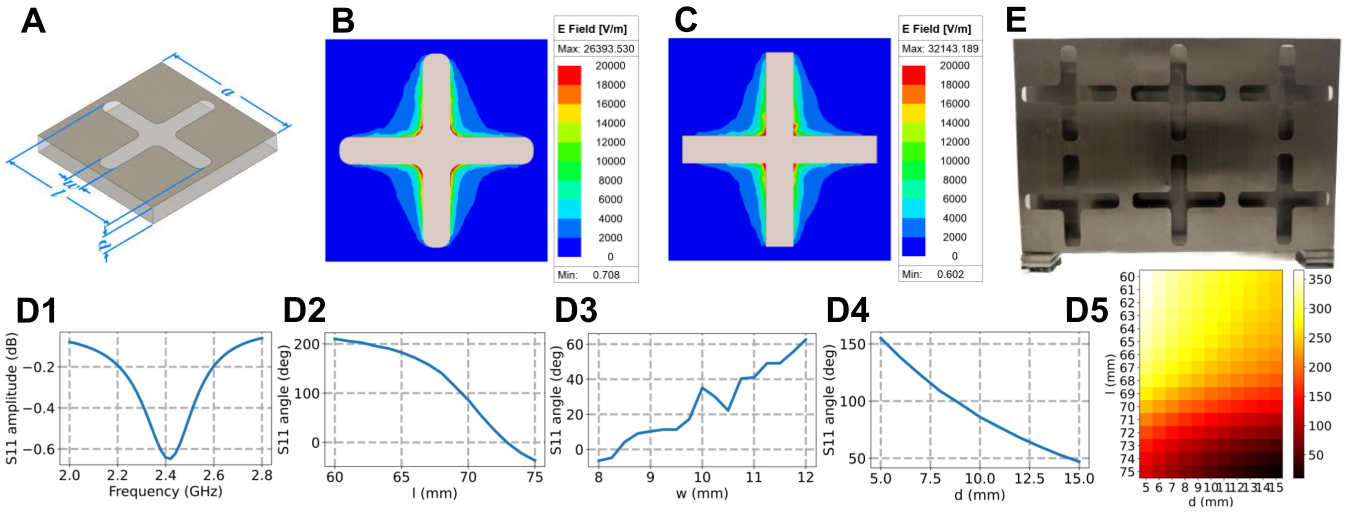

Figure 6: Metasurface design: (A) We design the element to be a cross with rounded corners. The design enables a small geometry while preventing burning; (B) By rounding the corners, the electric field is evenly distributed along the edges, which greatly reduces the risk of burning; (C) If the corners are not rounded, a large electric field could cumulate at the corners, causing danger; (D) The metasurface resonates at the 2.45 GHz range. The metasurface provides wide-range phase transition at the 2.45 GHz frequency; (E) The fabricated metasurface plate.

(1) It contains large gaps between metals to ensure safety; (2) Fabrication of the simple pattern using laser cutting is accurate and does not create rough edges after sanding, and thus prevents sparkling; (3) The overall thin metal sheet structure is more rigid and is less likely to be bent or damaged. In short, the design allows safe, cheap, and robust operation inside the oven. Figure 6(B) and (C) compare the electric field concentration with and without rough edges. Rounding edges reduces the maximum electric field intensity by 1/4 over the version without round edges.

The element design involves the following four tunable parameters: the overall length of the element a, the length of the cross l, the width of the cross w, and the distance between the cross element and the second metal layer d. To tune the metasurface, since the microwave oven chamber is of fixed size, we also fix the value of a to ensure that the metasurface covers one full side of the chamber, while leaving a 10 mm space for moving. As shown in Figure 6(D1), our final unit cell pattern results in an S11 peak at around 2.45 GHz, indicating an increase in the induced current of the metasurface, which is a sign of resonance. Figure 6(D2-D4) shows that by tuning the three parameters separately, l can change phase by up to 210-degree, and w and d can change the phase of the reflected wave by 65 degrees and 100 degrees, respectively. By optimizing the three parameters together, the metasurface can enable 2π phase tuning. Figure 6(D5) shows that by jointly tuning d and l, the metasurface has near 2π phase change.

Initialization based on the requirement of standing waves: We design a metasurface, which is placed parallel to the oven wall opposite the magnetron. Ideally, we want to tune standing waves inside a microwave oven for efficient heating of food. The basic idea of the tuning process is to find a good starting point where a simplified standing wave model yields a peak efficiency. MicroSurf considers two reflective surfaces, which are the metasurface and the opposite wall. Assuming the two reflective surfaces are lossless, the condition for the standing wave to form optimally is that the distance between the two surfaces is an integer multiplier of $\lambda/2$, where λ is the microwave wavelength. We use the standing wave condition to initialize the metasurface. Since we can not alter the microwave oven geometry, we use a phase offset realized by the metasurface to achieve the desired distance. Therefore, we initialize the phase offset of the metasurface such that the total traversed path from the magnetron to the metasurface on the opposite side plus the phase offset introduced by the metasurface is equal to an integer number of half wavelength. We use this insight to initialize the parameters w, l, d and the distance between the metasurface and microwave wall, b.

Further refinement using HFSS: The metasurface element needs to be optimized for each microwave oven chamber to achieve high efficiency. There are several reasons that the metasurface element needs to be further refined: (1) each microwave oven model operates in a slightly different frequency, as depicted in Sec 4; (2) the geometry of the microwave oven chamber is not an ideal cavity resonator, and

therefore the initialized starting point is not perfect for energy maximization; (3) the oven chamber is usually of 2-3λ size, which does not provide a fully far-field environment; (4) the metasurface elements are designed as if they formed an infinite array in the 2D plane, but in practice they have only a small number of elements due to the limited space. Therefore, the prior calculations are not accurate enough.

Considering such limitations, we further refine our metasurface design using HFSS. We take a reference food object: a beaker with around 60 mL water as a reference object to be heated. To maximize energy efficiency, we aim at maximizing the overall EM power absorbed by the water. The parameter space is defined as $\mathcal{P} = \{w, l, d, b\}$. The objective can be mathematically defined as follows.

$$\max_{\mathcal{P}} \quad \int_V L(x, y, z)\mathrm{d}v, \tag{2}$$

where $L(x, y, z)$ represents the dielectric loss density at point (x, y, z) and is integrated over the region V. Since water is the main EM energy absorption material in food at the 2.45 GHz range [21] and has the largest heat capacity, which leads to slower temperature increase than other food, it is an ideal reference object to measure the heating efficiency and uniformity of MicroSurf.

We use the Ansys Electronics HFSS's gradient-based method. The optimizer calculates the gradient of the objective function and descends/ascends towards the direction defined by the gradient at that point. When the difference between two iterations is within 0.2%, the optimization stops.

5.3 Uniform Heating

In most cases of microwave heating, we require that the food is heated both quickly and uniformly. A natural way to enforce uniformity is to minimize variance or adding the variance as a regularization term in the objective. However, these objectives do not work well because (1) Simply minimizing the variance would cause a minimization of the energy inside the optimization region. (2) The factor that controls the variance regularization is a hyperparameter that is difficult to set to balance the tradeoff between efficiency and uniformity. Instead, MicroSurf proposes slicing the food region into multiple pieces and maximizing the minimum absorbed energy in those pieces. We can adapt the size of each slice according to the granularity of the intended uniformity. We have optimized the metasurface element design for each model in Sec. 5.2 to maximize efficiency inside the chamber. We then use the metasurface element to ensure that uniformity optimization works for different geometries of food. In this case, MicroSurf searches for the placement and air gap between the two layers of the metasurface that optimizes our objective. We envision that the placement and air gap can be realized by connecting a small step motor to the metasurface.

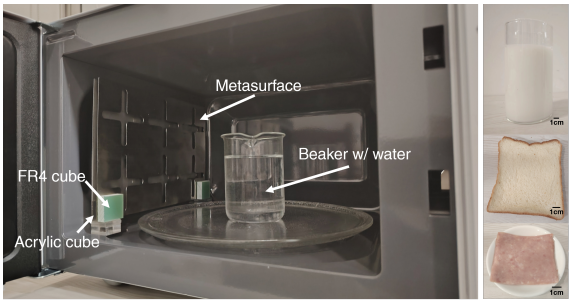

Figure 7: Setup of our experiment environment. On the left, a metasurface is placed, with optimized positions. Foods evaluated are milk, bread, and ham.

The optimization parameter space is defined as $\mathcal{P}_u = \{d, b\}$. As the food is sliced into different non-overlapping slices, denoted by $V_1, V_2, \cdots, V_N$, the objective can be formally written as follows.

$$\max_{\mathcal{P}_u} \quad \min_{n=1,2,\cdots,N} \int_{V_n} L(x, y, z)\mathrm{d}v \tag{3}$$

The optimization result specifies both the design and placement of the metasurface. Therefore, for each type of food, the metasurface can be placed at appropriate locations to achieve uniform heating. The optimization for each food type takes 24 hours on a desktop with 64 GB RAM and i9-12900K CPU. For a set of popular food types, we can optimize once and save the results, so the optimization time is acceptable.

5.4 Other objectives

MicroSurf's metasurface design and optimization are also suitable for other objectives. To realize more complex objectives, two or more metasurfaces can be used and jointly optimized. We showcase a heating example of selectively heating the four corners of bread with two metasurfaces in Section 7. The objective function is defined as maximizing the temperature in a selected area V_s inside the bread. Since there are two metasurfaces, the optimization space is defined as $\mathcal{P}_i = \{d_i, b_i\}, i = 1, 2$, where d_i and b_i are the air-gaps and placements, respectively. The optimization can be formally written as

$$\max_{\mathcal{P}_1, \mathcal{P}_2} \quad \int_{V_s} L(x, y, z)\mathrm{d}v. \tag{4}$$

We already see significant benefits in using two metasurfaces, but this framework can be extended to support more metasurfaces.

6 Implementation

Metasurface fabrication & assemblage: The metasurface is fabricated using 1.0 mm-thick Cr-304 stainless steel. The metasurface is two-layered. The first layer consists of hollow patterns displayed in Figure 6(A), which is fabricated using

laser cutting. The second layer is a full 1.0mm-thick Cr-304 stainless steel sheet. The sheet is of size 140×210 mm, with a 70×70 mm element size.

To assemble the metasurface, we use small acrylic cubes of size 20×20 mm with different thicknesses as an accurate spacing material between two layers of metasurfaces. The acrylic cubes are installed on the four corners of the metasurfaces. Since they are far away from the resonance element which is the cross-region, there is no significant temperature increase in the metasurface and cube. Moreover, two acrylic cubes of size $20 \times 20 \times 12$ mm are installed as the stand for the metasurface. Furthermore, two FR-4 cubes of size $25 \times 25 \times 8$ mm are installed on the lower two corners to balance the weight.

As shown in Figure 7, we place the metasurface on the left side of the microwave oven, parallel to the boundary. The placement of the metasurface is optimized according to different objectives. Depending on the scenario, we either heat the glass plate or food placed on the glass plate. Then we take out the heating target and take a thermal picture of the target.

Software: We use Ansys Electronics HFSS 2022 R2 to calculate the EM field inside the microwave oven with our established oven model. One can also use other simulation software, such as CST Microwave Studio or COMSOL, and use our refinement flows and optimization flows to find a simulation result that fits well with the measurement results. We use Python and PyAEDT to control the simulation program and perform detailed refinement. We use the simulated annealing algorithm in detailed refinement from Neural Network Intelligence (NNI) [24] for optimization.

7 Evaluation

7.1 Evaluation methodology

We evaluate our modeling and optimization using commodity microwave ovens. We use 4 microwave ovens from four different brands: Galanz, Midea, Panasonic, and Whirlpool, shown in Figures 4(B1-E1). All experiments are repeated five times and the average of the experiments is used for comparison. The thermal images all have been manually cut to preserve the object region and then scaled and rotated to the same size and position for comparison.

7.2 Impact of optimization objectives and microwave ovens

We heat water in a beaker for 30 seconds and compare the resulting temperature with and without our optimization. The baseline is the existing heating method with a rotating plate and without a metasurface, while our approach optimizes both the design and placement of a metasurface to maximize the total energy or minimum energy in a region without a rotating plate.

Figure 8 shows the infrared pictures, temperature changes at different heights, temperature change distribution, and standard deviation for Galanz, Midea, Panasonic, and Whirlpool microwave ovens, respectively. In Figure 8(E1-E4) box plot, the orange line in the middle corresponds to the average, the box corresponds to the 25%–75% temperature range, and the outer line corresponds to the 5%–95% temperature range. Our approach that maximizes the average temperature leads to 2-4°C higher temperature than the baseline for the corresponding microwave ovens, respectively. Our approach that maximizes the minimum temperature reduces the standard deviation to 1/5-1/3 of that of the rotating plate alone for the first three microwave ovens without decreasing the average temperature. The Whirpool microwave oven is relatively uniform with a rotating plate, but with our metasurface, the average temperature is 1°C higher and the temperature is more evenly distributed. These results demonstrate our approach is effective in optimizing the specified objective across multiple microwave ovens.

7.3 Impact of heating objects

We further compare the resulting temperature after heating different targets: bread, meat slice, and milk. The foods are shown in Figure 7. The foods are heated inside the Galanz microwave oven. The placement of metasurfaces is optimized for common food shapes (*e.g.*, lunchbox [28] and short/tall glass), allowing them to accommodate various types and shapes of food. For different food shapes and sizes, users simply reposition the metasurface prior to heating, which could be accomplished by selecting a microwave's heating mode, which would slide the metasurface to the right position.

For milk in Figure 9(A1-F1) that is poured into a 15-cm glass, the temperature increases from 15.5 to 17.5°C when we optimize the average temperature. The standard deviation decreases from 3.2 to below 1 when we use the uniform objective. The results show that when heating a tall object, the metasurface can provide efficiency and uniformity at the same time.

For bread, as shown in Figure 10(A1-F1), our approach also demonstrates both uniformity gain and efficiency gain. Without metasurface and with the rotating plate, the bread only has an average temperature increase of 35°C. Rotation significantly decreases the average temperature because the bread consists of a lot of small holes. During rotation, the holes contact with air and lose heat. By maximizing the temperature, the metasurface provides 10°C higher temperature. The uniform heating objective effectively prevents heat from being accumulated at the edges as shown in Figure 10(A1,B1). Uniform heating not only reduces the standard deviation from 4.2°C to 3.5°C, but also provides a 2.5°C temperature

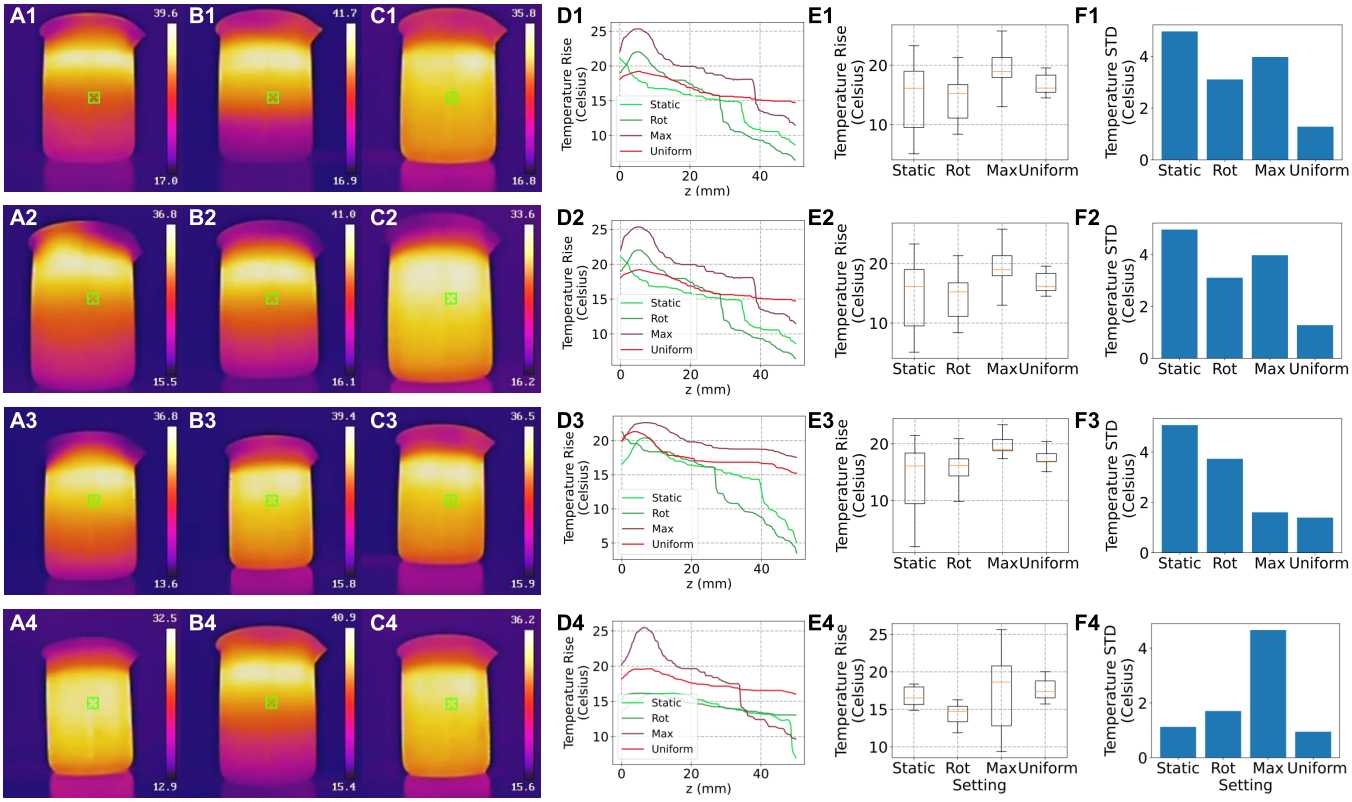

Figure 8: Experiment with a metasurface, in 4 microwave ovens of different models: (1) Galanz, (2) Midea, (3) Panasonic, (4) Whirpool; and 4 settings: (A) Heating without metasurface, without rotating plate (Static) or with rotating plate (Rot); (B) Metasurface to maximize total energy inside water (Max); (C) Metasurface to make the water temperature uniform (Uniform); (D) Temperature distribution on the Z (vertical) axis. (E) The box plot shows that the average temperature (red line) for *maximizing temperature objective* is 2-4°C higher than baseline, while *uniforming temperature objective* does not lose efficiency compared to baseline. (F) The temperature standard deviation shows that the variance for uniforming temperature is much lower than the baseline.

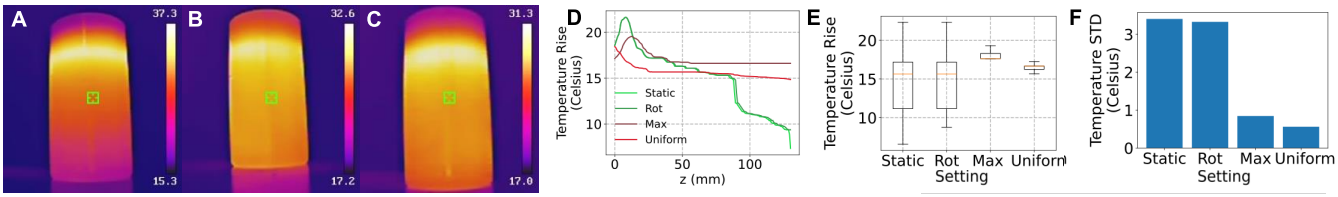

Figure 9: Experiment with a tall glass of milk: (A) Without metasurface; (B) Metasurface maximizes energy; (C) Metasurface uniforms heat; (D) Temperature distribution on the Z (vertical) axis; (E) When maximizing energy, the temperature is 2 higher; (F) With uniform heating, the standard deviation of temperature greatly decreases without metasurface.

increase. There is still temperature deviation in the small holes of the bread, which is inevitable.

For meat slices, a common problem of microwave ovens is that the edge of the meat heats up much more quickly than the center, as shown in Figure 10(A2). This causes the meat to be overheated at the edges while the center remains uncooked. With the metasurface and the turner, as shown in Figure 10(C2), the temperature is more uniformly spread into the center of the meat. The standard deviation also shows a decrease from 13°C to 3°C for the meat slice. When using the metasurface without the turner, the metasurface also successfully decreases the standard deviation from 13°C to 6°C.

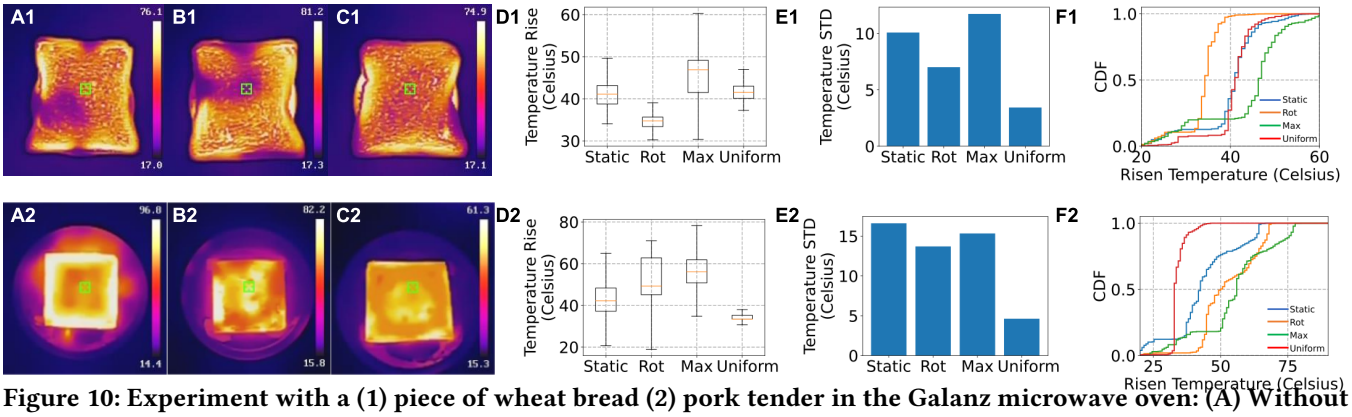

Figure 10: Experiment with a (1) piece of wheat bread (2) pork tender in the Galanz microwave oven: (A) Without metasurface; (B) Metasurface maximizes energy; (C) Metasurface uniforms heat; (D) Box plot of temperature shows with uniform heating, the standard deviation of temperature greatly decreases without metasurface; (E) When maximizing energy, the temperature is 2°C/7.4°C/8°C higher; (F) CDF of temperature.

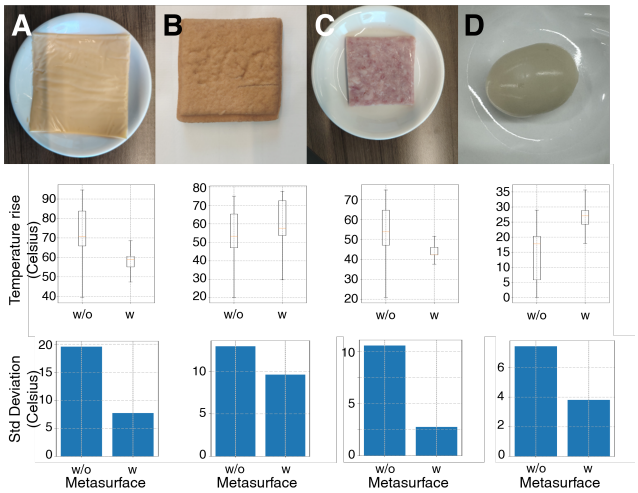

Figure 11: Generalizability to other types of food shows improvement in heating uniformity.

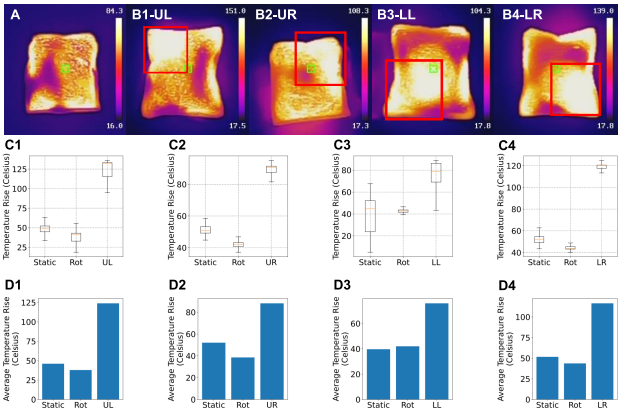

Figure 12: Heat four different corners of a bread: (A) Heating without metasurface; (B1) Upper-left corner; (B2) Upper-right corner; (B3) Lower-left corner; (B4) Lower-right corner. (C1)-(C4) shows the box plot of temperature rise at the desired region. (D1)-(D4) shows the average temperature rise at the desired region.

7.4 Generalizability

We heat other food of similar sizes with the same optimization parameters. We test the standard cube-sized food to evaluate the impact of different food materials on the performance of the metasurface. We use the same metasurface and metasurface positions as those used for ham and bread since they have a shape similar to that of the ham and bread. We use the uniform heating objective using the max-min optimization. When heating cheese for 5 seconds in Figure 11A, the standard deviation of the temperature decreases from 16°C to 8°C. For bean curd (Figure 11B), it has 3°C average temperature increase and standard deviation decrease from 14°C to 10°C from 30-second heating. For frozen meat (Figure 11C), the standard deviation decreases from 15°C to 3.5°C, which shows the advantage of MicroSurf to uniformly defrost meat. Finally, the average temperature of eggs (Figure 11D) increases by 8°C its temperature deviation decreases from 8.5°C to 6°C.

7.5 Impact of different heating regions

We further compare the resulting temperature under different heating regions: left top, right top, left bottom, and right bottom. The bread is placed on the plate and we aim to maximize the energy of the four corners. Compared with the case without metasurface as shown in Figure 12(A), Figure 12(B1-B4) show the infrared image after heating a slice of bread for 30 seconds. It is evident the hot part matches with the optimization objective. Figure 12(C1-C4, D1-D4) further compares the average temperature inside the specified

heating regions. As we can see, our optimization leads to 75, 35, 35, and 55-degree increase in the temperature when heating the upper-left, upper-right, lower-left, and lower-right, respectively.

8 Related Work

Our work is related to metasurface technology and microwave oven technology.

Metasurface technology: A metasurface is a 2D structure that can provide fine-grained control on the electromagnetic (EM) wave, including the phase, amplitude, and polarization of EM wave. Existing metasurface solutions focus on enhancing wireless communication and sensing [32, 36]. For example, reconfigurable metasurfaces have been widely used for the dynamic control of wireless communication channels, such as shaping the wavefront [42], controlling polarization [2, 13], and tuning frequency [46]. These metasurfaces can be used to dynamically optimize the communication link according to multipath fading and interference [6]. Reconfigurable metasurfaces are relatively expensive. For example, mmWall [7] costs around \$10K for 28×76 elements.

Passive metasurfaces have also been explored in wireless communication [20, 27, 29, 39, 45], which are much cheaper. For example, milliMirror [29] costs \$15 for 80×80 elements. However, once manufactured, such systems are generally not reconfigurable. Despite considerable work on metasurface, to our knowledge, our work is the first system that uses low-cost passive metasurfaces to enhance energy distribution in a microwave oven and demonstrates its effectiveness in a commercial microwave oven.

Microwave oven: Several complementary technologies have been developed to improve energy distribution in microwave ovens. Many microwave ovens employ a stirrer, a fan-like rotating device that helps distribute heating inside a microwave more evenly and reduces hot spots. Another widespread technique involves using a rotating turntable to expose different sections of the food to the microwave transmitter, promoting more uniform heat distribution. Some researchers focus on optimizing the shape of the microwave oven cavity to improve heating uniformity (*e.g.*, using techniques such as the Arbitrary Lagrangian-Eulerian method) [44]. Multi-level cooking racks are also available in some microwave ovens, enabling users to place food at different levels inside the oven for more even cooking. Inverter microwaves provide more consistent heating through a continuous power supply. Sensors can be used to monitor humidity and temperature inside the oven, adjusting cooking time and power levels as needed. Some modern microwave ovens utilize multiple energy distribution points to direct microwaves toward specific regions, further reducing hot spots. Additionally, some researchers control the rotation and/or output frequency to change the field pattern [14]. Solid-state microwave ovens have also been developed, which can vary output frequency and phase based on feedback power to interfere with the standing wave pattern and achieve power convection [10]. SDC [15] develops a programmable turntable and controls the turntable based on high-resolution heat sensing. While it is effective in increasing the temperature of the target object using a closed-loop design, it requires significant modification to the microwave (*e.g.*, adding a neon light, camera, programmable turntable, and controller), and incurs significant cost and deployment overhead. Moreover, their approach controls the EM field only in 2D instead of 3D.

Our passive metasurface-based approach is complementary to these approaches and can be combined with the previous approaches to further enhance the uniformity of energy distribution. Moreover, as shown in our evaluation, it has several distinct benefits: (i) it is easy to use by simply placing the metasurface at designated locations, (ii) it is low-cost (\$4 when custom made and much lower with mass production), (iii) it is effective (*i.e.*, improve the evenness of energy distribution by decreasing the standard deviation by 50% and increasing the temperature at the target region by 5°C-8°C), and (iv) it is flexible (*i.e.*, can support a variety of optimization objectives).

9 Conclusion

We develop the first system that applies a low-cost passive metasurface to enhance the energy distribution inside a microwave oven. Our system consists of modeling microwave heat distribution and optimizing metasurface design and placement. We evaluate its performance using different commodity microwave ovens and show its effectiveness in supporting various optimization objectives across different microwave ovens and food types. Our design is simple, practical, and easy to use. A user can simply choose her desired heating pattern by placing the metasurface at an appropriate position. As part of our future work, we plan to further enhance the accuracy of our model and the performance of our optimization, and evaluate our design across more microwaves. The high-level approach developed in Microsurf goes beyond heating food and can be potentially applied to microwave chemistry, material processing, actuating soft robots [37, 41], and industry applications [3, 22, 23], which we are interested in exploring as part of our future work.

Acknowledgments

We are grateful to anonymous reviewers for their constructive comments, and appreciate the shepherd's meticulous revision suggestions. We acknowledge support from the NSF (2106921, 2030154, 2007786).

References

[1] Cooking with microwave ovens. https://www.fsis.usda.gov/food-safety/safe-food-handling-and-preparation/food-safety-basics/cooking-microwave-ovens.

[2] O. Akgol, E. Unal, O. Altintas, M. Karaaslan, F. Karadag, and C. Sabah. Design of metasurface polarization converter from linearly polarized signal to circularly polarized signal. *Optik*, 161:12–19, 2018.

[3] S. M. Allan. Energy saving glass lamination via selective radio frequency heating. Technical report, Ceralink Inc., Troy, NY, 2012.

[4] G. Caloz, M. Dauge, E. Faou, and V. Péron. On the influence of the geometry on skin effect in electromagnetism. *Computer Methods in Applied Mechanics and Engineering*, 200(9-12):1053–1068, 2011.

[5] H. Chen, W.-B. Lu, Z.-G. Liu, and M.-Y. Geng. Microwave programmable graphene metasurface. *Acs Photonics*, 7(6):1425–1435, 2020.

[6] L. Chen, W. Hu, K. Jamieson, X. Chen, D. Fang, and J. Gummeson. Pushing the physical limits of IoT devices with programmable metasurfaces. pages 425–438, Apr. 2021.

[7] K. W. Cho, M. H. Mazaheri, J. Gummeson, O. Abari, and K. Jamieson. mmwall: A steerable, transflective meta-material surface for nextg mmwave networks. In *Proc. of NSDI*, 2023.

[8] A. Datta and V. Rakesh. Principles of microwave combination heating. *Comprehensive Reviews in Food Science and Food Safety*, 12(1):24–39, 2013.

[9] C. Design. Successful induction heating of rcs billets. 2008.

[10] T. Forrister. Optimizing microwave ovens with solid-state rf cooking. https://www.comsol.com/blogs/optimizing-microwave-ovens-with-solid-state-rf-cooking/.

[11] B. S. Guru and H. R. Hiziroglu. *Electromagnetic field theory fundamentals*. Cambridge university press, 2009.

[12] W. Hardy and L. Whitehead. Split-ring resonator for use in magnetic resonance from 200–2000 mhz. *Review of Scientific Instruments*, 52(2):213–216, 1981.

[13] X. Huang, H. Yang, D. Zhang, and Y. Luo. Ultrathin dual-band metasurface polarization converter. *IEEE Transactions on Antennas and Propagation*, 67(7):4636–4641, 2019.

[14] M. Jiang, Z. T. T. Hong, and Y. Hu. A new microwave heating method via the combination of rotation and boundary movement. *Journal of Physics: Conference Series*, May 2021.

[15] H. Jin, J. Wang, S. Kumar, and J. Hong. Software defined cooking using a microwave oven. In *Proc. of ACM MobiCom*, 2019.

[16] S. Kamol, P. Limsuwan, and W. Onreabroy. Three-dimensional standing waves in a microwave oven. *American Journal of Physics*, 78(5):492–495, 2010.

[17] Y. B. Li, L. L. Li, B. B. Xu, W. Wu, R. Y. Wu, X. Wan, Q. Cheng, and T. J. Cui. Transmission-type 2-bit programmable metasurface for single-sensor and single-frequency microwave imaging. *Scientific reports*, 6(1):23731, 2016.

[18] Z. Li, X. Tian, C.-W. Qiu, and J. S. Ho. Metasurfaces for bioelectronics and healthcare. *Nature Electronics*, 4(6):382–391, 2021.

[19] L. Liu, X. Zhang, M. Kenney, X. Su, N. Xu, C. Ouyang, Y. Shi, J. Han, W. Zhang, and S. Zhang. Broadband metasurfaces with simultaneous control of phase and amplitude. *Advanced materials*, 26(29):5031–5036, 2014.

[20] R. Ma, S. Zheng, H. Pan, L. Qiu, X. Chen, L. Liu, Y. Liu, W. Hu, and J. Ren. Automs: Automated service for mmwave coverage optimization using low-cost metasurfaces. In *Proceedings of the 30th Annual International Conference on Mobile Computing and Networking*, pages 62–76, 2024.

[21] S. Ma, X. Zhou, X. Su, W. Mo, J. Yang, and P. Liu. A new practical method to determine the microwave energy absorption ability of materials. *Minerals Engineering*, 22(13):1154–1159, 2009.

[22] A. K. Mandal and R. Sen. An overview on microwave processing of material: a special emphasis on glass melting. *Materials and manufacturing processes*, 32(1):1–20, 2017.

[23] A. Metaxas, , and R. J. Meredith. *Industrial microwave heating*. Number 4. IET, 1983.

[24] Microsoft. Neural Network Intelligence, 1 2021.

[25] A. J. Morgan, J. Naylon, S. Gooding, C. John, O. Squires, J. Lees, D. A. Barrow, and A. Porch. Efficient microwave heating of microfluidic systems. *Sensors and Actuators B: Chemical*, 181:904–909, 2013.

[26] J. M. Osepchuk. Microwave power applications. *IEEE Transactions on Microwave Theory and Techniques*, 50(3):975–985, 2002.

[27] H. Pan, L. Qiu, B. Ouyang, S. Zheng, Y. Zhang, Y.-C. Chen, and G. Xue. Pmsat: Optimizing passive metasurface for low earth orbit satellite communication. In *Proceedings of the 29th Annual International Conference on Mobile Computing and Networking*, pages 1–15, 2023.

[28] C. Pluim, D. Powell, and D. Leahy. Schooling lunch: Health, food, and the pedagogicalization of the lunch box. *Educational dimensions of school lunch: Critical perspectives*, pages 59–74, 2018.

[29] K. Qian, L. Yao, X. Zhang, and T. N. Ng. Millimirror: 3d printed reflecting surface for millimeter-wave coverage expansion. In *Proceedings of the 28th Annual International Conference on Mobile Computing And Networking*, MobiCom '22, page 15–28, New York, NY, USA, 2022. Association for Computing Machinery.

[30] H. Ren. A light-programmable metasurface. *Nature Electronics*, 3(3):137–138, 2020.

[31] R. Rosa, P. Veronesi, and C. Leonelli. A review on combustion synthesis intensification by means of microwave energy. *Chemical Engineering and Processing: Process Intensification*, 71:2–18, 2013.

[32] e. a. S. Sasikala; K. Karthika; K. Kavitha; S. Arun Kumar; S. Adithya; V. Harisivabharath; V. Ohmprakash. Gain enhancement using metasurface in antenna design for advanced wireless communication – a short review. *2023 2nd International Conference on Advancements in Electrical, Electronics, Communication, Computing and Automation (ICAECA)*, 2023.

[33] A. Sangster, K. Sinclair, M. Desmulliez, and G. Goussetis. Open-ended microwave oven for flip-chip assembly. *IET microwaves, antennas & propagation*, 2(1):53–58, 2008.

[34] L. Shao and W. Zhu. Electrically reconfigurable microwave metasurfaces with active lumped elements: A mini review. *Frontiers in Materials*, 8:689665, 2021.

[35] P. Sharma, L. Lao, and G. Falcone. A microwave cavity resonator sensor for water-in-oil measurements. *Sensors and Actuators B: Chemical*, 262:200–210, 2018.

[36] N. Shlezinger, G. C. Alexandropoulos, M. F. Imani, Y. C. Eldar, and D. R. Smith. Dynamic metasurface antennas for 6g extreme massive mimo communications. *IEEE Wireless Communications*, 28(2):106–113, 2021.

[37] Y. Song, M. Zadan, K. Misra, Z. Li, J. Wang, C. Majidi, and S. Kumar. Navigating soft robots through wireless heating. In *2023 IEEE International Conference on Robotics and Automation (ICRA)*, pages 2598–2605. IEEE, 2023.

[38] J. Sun, W. Wang, and Q. Yue. Review on microwave-matter interaction fundamentals and efficient microwave-associated heating strategies. *Materials*, 9(4):231, 2016.

[39] T. A. Tsiftsis, C. Valagiannopoulos, H. Liu, A.-A. A. Boulogeorgos, and N. I. Miridakis. Metasurface-coated devices: A new paradigm for energy-efficient and secure 6g communications. *IEEE Vehicular Technology Magazine*, 17(1):27–36, 2022.

[40] R. Vadivambal and D. Jayas. Non-uniform temperature distribution during microwave heating of food materials—a review. *Food and bioprocess technology*, 3:161–171, 2010.

[41] J. Wang, Y. Song, M. Zadan, Y. Shen, V. Chen, C. Majidi, and S. Kumar. Wireless actuation for soft electronics-free robots. In *Proceedings of*

the 29th Annual International Conference on Mobile Computing and Networking, Mobicom'23, pages 1–16, 2023.

[42] Q. Yang, J. Gu, D. Wang, X. Zhang, C. O. Zhen Tian, R. Singh, J. Han, , and W. Zhang. Efficient flat metasurface lens for terahertz imaging. *Opt. Express 22, 25931-25939 (2014)*, 2014.

[43] J. Zhang and W. Zhu. Graphene-based microwave metasurfaces and radio-frequency devices. *Advanced Photonics Research*, 2(11):2100142, 2021.

[44] J. Zhou, Y. Wang, and X.-Q. Yang. Shape optimization of microwave cavity using arbitrary lagrangian–euler method to improve the heating uniformity. In *IEEE Transactions on Microwave Theory and Techniques*, March 2022.

[45] B. O. Zhu and Y. Feng. Passive metasurface for reflectionless and arbitary control of electromagnetic wave transmission. *IEEE Transactions on Antennas and Propagation*, 63(12):5500–5511, 2015.

[46] H. L. Zhu, X. H. Liu, S. W. Cheung, and T. I. Yuk. Frequency-reconfigurable antenna using metasurface. *IEEE Transactions on Antennas and Propagation*, 62(1):80–85, 2014.